

# Transfer Printing Process of Bio-Based Nylon 56 and Cotton Interwoven Fabrics

Runshan Chu<sup>1</sup>, Yanbo Zhang<sup>1</sup>, Ling Li<sup>1</sup>, Tieling Xing<sup>1,2,\*</sup> and Guoqing Chen<sup>1,\*</sup>

<sup>1</sup>National Engineering Laboratory for Modern Silk, College of Textile and Clothing Engineering, Soochow University, 199 Renai Road, Suzhou 215123, Jiangsu, China

<sup>2</sup>National Innovation Center of Advanced Dyeing and Finishing Technology, Tai'an 271000, China

**Abstract:** Using Annosol Reactive Blue DS dye as the colorant, an inkjet printing ink was developed, and its rheological properties and dynamic surface tension were evaluated for its use in dry heat transfer printing of patterns on bio-based nylon 56 and cotton interwoven fabrics. In particular, the effects of the dry heat transfer printing parameters on the printing properties of the ink on bio-based nylon 56 and cotton interwoven fabrics were investigated. The results revealed that the optimal parameters of the dry heat transfer printing of the custom-produced ink on bio-based nylon 56 and cotton interwoven fabrics are as follows: hot pressing at 130 °C under 3MPa pressure, steamer at 102 °C, and saturated steaming for 15min. The color fastness to both soap wash and rubbing of the bio-based nylon 56 and cotton interwoven fabrics dyed with Annosol Reactive Blue DS through dry heat transfer printing were determined to be of grades 3–4 and above, meeting the color fastness requirements of printed fabrics.

**Keywords:** Dry heat transfer printing, Reactive dye, Bio-based nylon 56, Cotton.

## 1. INTRODUCTION

Theoretically, bio-based nylon products can replace petroleum-based products. Simultaneously, bio-based nylon can reduce the consumption of petroleum resources, overcoming the problem of raw material shortages in petroleum-based product development, and has the advantages of low carbon emission, environmental protection, and sustainable development. Accordingly, bio-based nylons such as PA11, PA1010, PA56, PA6, and PA66 have been developed, and some of them have been industrialized [1-7]. The research on bio-based nylon is focused on its renewability, and its production process routes are mainly focused in two directions. The first is to produce raw nylon materials using renewable sugars, such as starch and glucose, using microbial technologies or chemical methods, such as the synthesis of adipic acid under the catalysis of *Escherichia coli* and the synthesis of caprolactam and 1,5-pentanediamine from lysine by the fermentation of sugar compounds [1]. The second is to use natural and renewable oil products (e.g., castor oil, oleic acid, and linoleic acid) to prepare nylon raw materials through a series of chemical transformations, including transesterification and high-temperature cracking of animal and vegetable oils,

such as castor oil and eleven  $\omega$ -amino acids, through saponification, oxidation, and cracking to produce azelaic acid.

Bio-based nylon 56 is obtained by the polymerization of adipic acid and pentanediamine produced by the biological fermentation of lysine. In recent years, the technology for producing pentanediamine through biological methods has matured significantly, and bio-based nylon 56, which uses pentanediamine as a raw material, has attracted considerable attention as a new nylon material. Biomass raw materials have the advantages of being renewable, partially biodegradable, and recyclable, and provide good environmental benefits; they reduce environmental pollution by significantly reducing carbon emissions during production. The research and development of the biomass technology is of great significance for the utilization of renewable resources [8, 9]. The preparation of the transfer printing paper involves coating a modified paste on the surface of paper and then patterning the ink on the transfer printing paper using an inkjet printer to form a floral pattern. Dry heat transfer printing involves tightly fitting the transfer paper and fabric at a certain temperature and pressure, followed by the dissolution, transfer, and fixing of the dye on the fabric with the aid of steam. Finally, the fabric is peeled off the transfer paper and washed with water [10].

Li *et al.* [11, 12] studied the transfer printing of an ink formulation on silk using transfer paper; the ink was

\*Address correspondence to this author at the National Engineering Laboratory for Modern Silk, College of Textile and Clothing Engineering, Soochow University, 199 Renai Road, Suzhou 215123, Jiangsu, China; Tel: 86-512-67061152; E-mail: xingtieling@suda.edu.cn; chengguojiang@suda.edu.cn

prepared by mixing sodium alginate with highly substituted hydroxypropyl cellulose and sodium carboxymethyl cellulose as thickeners and water-soluble polyester as the hot-melt adhesive for printing patterns on silk fabric to achieve good color yield, fastness, and high pattern clarity. Miao used different thickeners for the dry heat transfer printing of cotton fabrics and found that the type of the thickener and moisture absorbent, and the content of nano SiO<sub>2</sub> significantly affect the clarity of the patterns formed on modified paper [13]. Zhang *et al.* developed a modified paste for transfer paper and studied the printing of a disperse/reactive dye via dry transfer printing onto polyester/cotton fabrics. The results indicated that upon selecting appropriate alkali agents and optimizing the alkali agent content, pressing temperature, and pressing time, a high color yield could be achieved on both polyester and cotton fabrics [14]. Ma *et al.* studied the dyeing performance and adsorption mechanism of an Eriofeast series of reactive dyes on nylon 56; the results revealed that the Eriofeast series of dyes exhibit both non-localized and localized adsorption on nylon 56, which is consistent with the composite adsorption mechanism of the Freundlich and Langmuir types [15].

Previously, our research group discovered that, when Annosol Reactive Blue DS (vinyl sulfone type) is used to dye bio-based nylon 56, the sensitivity of the dye to pH is low, and the dye facilitates a high dyeing depth even at solution pH of 7–9, because the vinyl sulfone group can covalently bond with the amino groups in nylon 56. Considering this, in the present study, we used Annosol Reactive Blue DS as the colorant and formulated an inkjet printing ink to explore the dry heat transfer printing process of the reactive dye-based ink on bio-based nylon 56 and cotton interwoven fabrics.

## 2. MATERIALS AND METHODS

### 2.1 Materials

Bio-based nylon 56 and cotton interwoven fabrics (100 gm<sup>-2</sup> each) supplied by Lianfa Co., Ltd. (China) and transfer printing paper (80 gm<sup>-2</sup>) provided by Changzhou Hanyuan New Printing Co., Ltd. (China) were used in this study.

Annosol reactive blue DS dyes are commercially available. Ethylene glycol, glycerol, triethanolamine, fatty alcohols, polyoxyethylene ether, and polyvinyl

pyrrolidone K-30 were of analytical grade. The soap flakes used in this study were of industrial grade.

## 2.2 PROCEDURE

### 2.2.1 Formulation of the Ink for Inkjet Printing

First, a mixture of 10% Anoxol blue DS, 10% ethylene glycol, 15% glycerol, 0.2% triethanolamine, 0.5% polyvinylpyrrolidone K-30, 0.4% fatty alcohol polyoxyethylene ether, and 63.9% deionized water was stirred to obtain a homogeneous suspension. Then, the resulting ink was filtered sequentially through 0.8, 0.45, and 0.2 μm filter membranes to obtain the ink suitable for inkjet printing.

### 2.2.2. Inkjet Printing

The transfer printing paper was cut into A4 sizes, and an Epson printer was used to print patterns and lines on the transfer printing paper using the formulated ink. Finally, the ink was allowed to dry naturally before further use.

### 2.2.3. Transfer Printing

The entire transfer printing process is illustrated in Figure 1, and the conditions for the major stages in the process are listed in Table 1.

## 2.3. Instrumentation and Characterizations

The viscosity of the ink was measured using a rotational viscometer (Rheolab QC Anton Paar China Co., Ltd., Austria). The dynamic surface tension of the ink was evaluated using a Kruss BP100 dynamic surface tensiometer at 20 °C. The speed and volume of the ink droplets were measured using a JetXpert ink droplet observation instrument. Each sample was analyzed 70 times, and a spray map of the ink droplets was obtained.

The K/S value of the fabric was determined using an Ultra Scan XE computer color-measuring and color-matching instrument. The test conditions were a D65 light source with a 10° viewing angle. The test fabric was folded into four layers, and the average value of four test results was obtained.

The fixation and penetration rates of the dye were calculated using Equation (1) and (2), respectively.

$$\text{Fixation rate} = (K/S)_f / (K/S)_{f0} \times 100\% \quad (1)$$

$$\text{Penetration rate} = (K/S)_b / 0.5 \times [(K/S)_b + (K/S)_f] \times 100\% \quad (2)$$

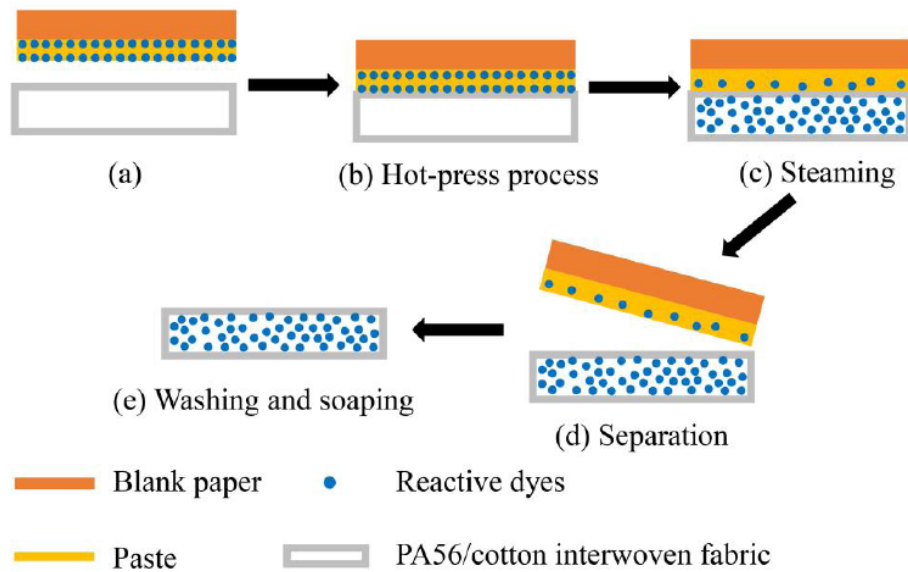


Figure 1: Schematic illustration of the transfer printing process.

Table 1: Transfer Printing Conditions

Stage of Printing	Conditions for Work	Instruments
(b) Adhesion	Pressure: 1–5 MPa, 90–140 °C, roller speed: 10 rev min <sup>-1</sup>	Transfer calendar, Rapid LC-250
(c) Steaming	Saturation steam: 75%, 5–30 min at 102 °C	Steaming machine, Real Color Dyeing Tech. Co., Ltd.(Shanghai)
(d) Separation	The transfer paper was peeled off the printed fabric	--
(e) Washing and soaping	4 min in cold water, 10 min at 90 °C in soap water	Oscillating water bath machine

Here,  $(K/S)_0$  refers to the front K/S value of the printed fabric before washing, and  $(K/S)_f$  and  $(K/S)_b$  refer to the front and back K/S values of the printed fabric after washing, respectively.

Lines with a width of 353 μm were edited on the computer and printed onto the fabric using an inkjet printer, and the widths of the warp and weft lines of the printed fabric were tested using the super depth of a field microscope (Keyence Co., Ltd., China).

The washing and rubbing fastness values of the printed fabrics were determined according to GB/T 3921-2008 and GB/T 3920-2008, respectively.

### 3. RESULTS AND DISCUSSION

#### 3.1. Properties of the Ink

##### 3.1.1. Ink Viscosity

The rheological properties of the custom-produced ink were evaluated using a Rheolab QC rotational

viscometer to examine the relationship between the shear stress, viscosity, and shear rate of the ink. Furthermore, the relationship between the ink viscosity and temperature was also examined at a constant shear rate.

Figures 2-(a) and 2-(b) show the shear rate-dependence of the shear stress and viscosity of the custom-produced ink at the temperature of 20 °C; the shear rate was varied from 150 to 1000 s<sup>-1</sup>. As shown, the shear stress of the ink is linearly related to the shear rate, and the viscosity does not change significantly with the increase in the shear rate, indicating that the custom-made ink exhibits the characteristics of a Newtonian fluid in this shear rate range [16].

The rheological properties of the ink affect its jetting performance, which in turn affects the quality of the patterns printed by inkjet printing. Figure 2-(c) shows the relationship between the viscosity of the ink and

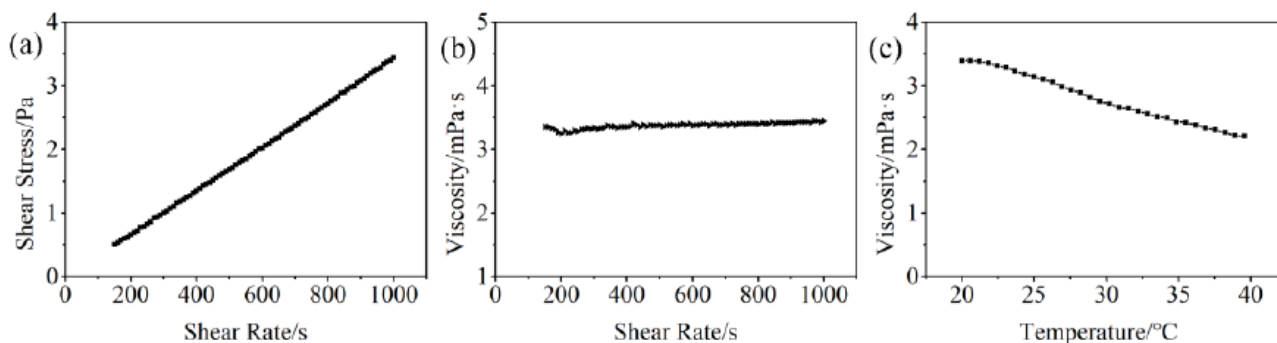


**Figure 2:** Rheological properties of the ink: (a) shear stress vs. shear rate, (b, c) dependence of the viscosity of the ink with shear rate and temperature, respectively.

temperature for the 20 to 40 °C range at a fixed shear rate of 60 s<sup>-1</sup>. The plot indicates that, as the temperature increases, the intermolecular forces weaken and the molecular mobility increases, resulting in decreased viscosity of the ink.

### 3.1.2. Dynamic Surface Tension of the Ink

Figure 3 presents the dynamic surface tension of the ink measured using a Kruss BP100 dynamic surface tensiometer at 20 °C. The surface tension of the ink first decreased rapidly with time and then slowly, and it finally tended to remain constant. The plateau value of the surface tension of the ink is 32.88 mN/m. The adsorption of surfactant molecules to the ink surface is a spontaneous process. As time progresses, the greater the adsorption efficiency of the surfactant molecules in the ink at the surface of the solution is, the faster the decrease in surface tension is.

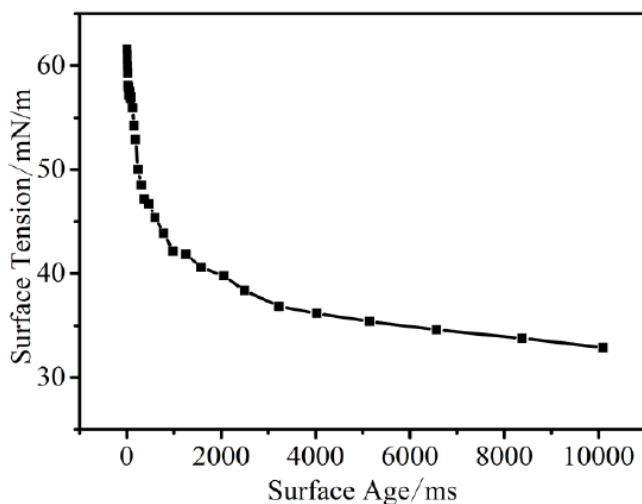


**Figure 3:** Dynamic surface tension curve of the ink developed for inkjet printing.

### 3.1.3. Process of Ink Droplet Formation

The ink used for inkjet printing was formulated by homogeneously mixing 10% Anoxol blue DS, 10% ethylene glycol, 15% glycerol, 0.2% triethanolamine, 0.5% polyvinylpyrrolidone K-30, 0.4% fatty alcohol polyoxyethylene ether, and 63.9% deionized water and then sequentially filtering the resulting solution through filtration membranes of decreasing pore sizes, viz., 0.8, 0.45, and 0.2 μm membranes. To monitor the process of ink droplet formation, the photographs of the ink droplet states were obtained every 5 μs between 20 and 70 μs, and the results are shown in Figure 4.

According to Figure 4, during 0–20 μs, the positive pressure above the nozzle acted on the ink inside the nozzle, causing it to spray out of the nozzle. At this point, the ink droplet appeared hemispherical or ellipsoidal. Over time, as the positive pressure above the nozzle continued to act on the ink, slender ink droplets were initially formed. Owing to the acceleration of the ink droplets, the velocity gradients of the different liquid layers differed, resulting in an increase in the speed and length of the ink droplets. During 25–30 μs, the negative pressure starting from above the nozzle reduced the downward velocity of the ink droplet. As the velocity of the droplet is also affected by the combined effect of its own gravity and surface tension, the ink inside the nozzle retracted upward, whereas the droplet head continued to move downward, causing the ink droplet to fracture at 30–35 μs. During 35–50 μs, the ink droplet separated from the nozzle, resulting in a droplet with a spherical front end and a thin strip at the tail end. Owing to the surface tension at the tail end, a downward acceleration occurs, causing the downward movement speed of the tail end to rapidly increase and eventually catch up with the speed of the front end of the ink droplet. Thus, the head and tail end were close to each other, and the length of the ink droplet

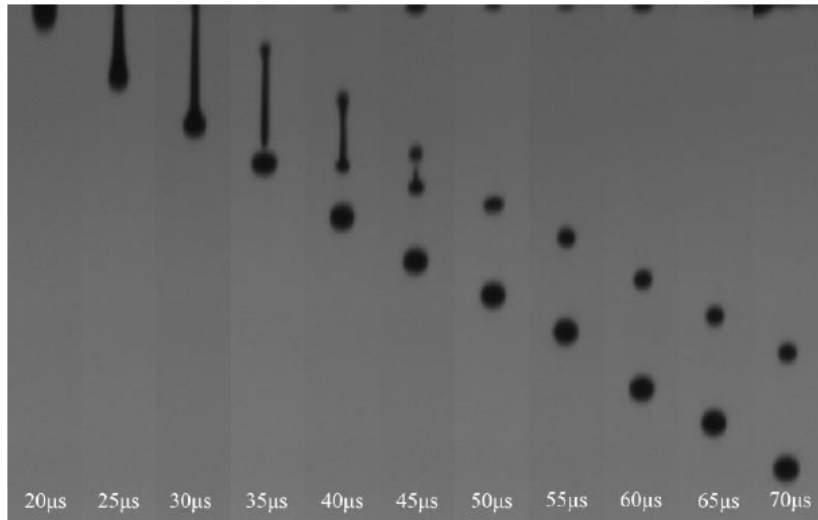


**Figure 4:** A series of snapshots illustrating the process of ink droplet formation.

decreased, resulting in a spherical ink droplet. Owing to the accumulation of the tail mass, its volume continues to increase, ultimately resulting in the formation of tail ink droplets, viz., satellite ink droplets.

For the ink system developed in this study, satellite ink droplets and main ink droplets gradually formed during 45–50  $\mu\text{s}$ . The satellite ink droplets cannot catch up with the main ink droplet and cannot recombine with it to form a single ink droplet [17, 18].

### 3.2. Optimization of the Transfer Printing Process

#### 3.2.1. Influence of the Hot-Pressing Pressure on the Printing Quality

In the process of hot pressing, the temperature was set to 110  $^{\circ}\text{C}$  and the pressure was varied, and steam was passed for 15 min through a steamer at a temperature of 102  $^{\circ}\text{C}$  to achieve a steam saturation of 75%. Here, the results obtained by varying the hot-pressing pressure is discussed. To optimize the process, the color strengths (K/S values) of the fabrics printed under different conditions were evaluated, the results are shown in Figure 5.

As shown in Figure 5, the K/S value of the printed fabric was the highest when the hot-pressing pressure reached 3 MPa. As the hot-pressing pressure was increased further, the K/S value of the printed fabric exhibited a decreasing trend; however, the change was small. The hot-pressing pressure affects the tightness of the adherence of the transfer printing paper and fabric. The fabric used in this test was thicker, and the hot-pressing pressure hardly affected the permeability of the ink. According to the results, in the transfer

printing process of bio-based nylon 56 and cotton interwoven fabric, a higher K/S value can be obtained using a hot-pressing pressure of 3 MPa.

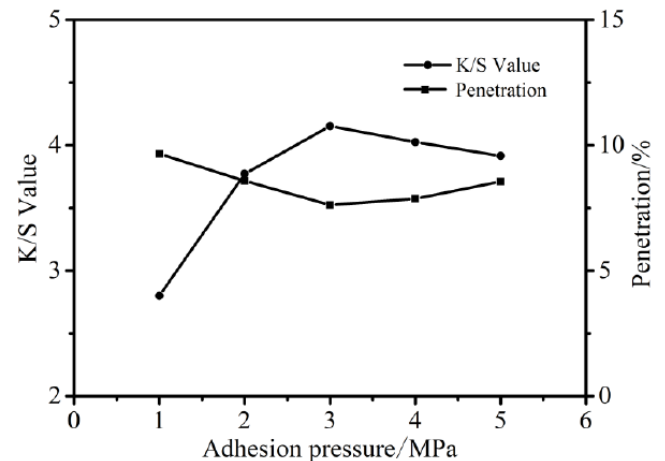


**Figure 5:** Effect of the hot-pressing pressure on the K/S value and ink permeability.

#### 3.2.2. Influence of Hot-Pressing Temperature on the Printing Quality

In the process of hot-pressing lamination, the hot-pressing pressure was set to 3 MPa and the hot-pressing temperature was varied; then, steam was passed for 15 min through a steamer at a temperature of 102  $^{\circ}\text{C}$  to achieve a steam saturation of 75%. The K/S value of the printed fabric was reduced to optimize the process, and the results obtained by varying the hot-pressing temperature are shown in Figure 6.

As shown in Figure 6, when the hot-pressing temperature was increased to 130  $^{\circ}\text{C}$ , the K/S value of the printed interwoven fabric reached the maximum

value. As the temperature was increased further to 140 °C, the K/S value of the interwoven fabric decreased, and the dye penetration rate increased gradually, but the variation range was small. This is probably because, as the temperature increases, the melting degree of the hot-melt adhesive on the transfer paper increases, and the bonding force between the fabric and transfer paper increases. When the hot-pressing temperature is 130 °C, the amount of dye penetrating the fabric increases because the permeability of the ink increases, and the front K/S value of the fabric decreases. Thus, in the transfer printing process of bio-based nylon 56 and cotton interwoven fabrics, a higher K/S value can be obtained using a hot-pressing temperature of 130 °C.

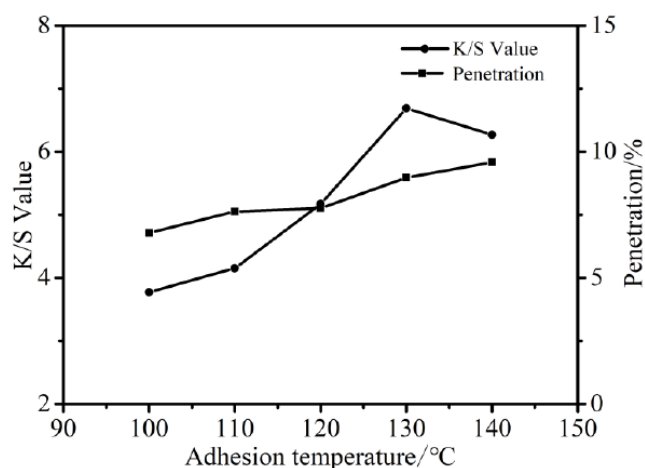


**Figure 6:** Effect of hot-pressing temperature on the K/S value and ink permeability.

### 3.2.3. Influence of the Steaming Time on the Printing Quality

Next, the effect of the steaming time on printing was evaluated. For this, the hot-pressing pressure and temperature were set to 3 MPa and 130 °C, respectively, and the interwoven fabric was attached to the transfer printing paper. Further, the steaming machine temperature was set to 102 °C, 75% steam saturation was achieved, and the steaming time was varied as 5, 10, 15, 20, and 30 min. To evaluate the effect of the steaming time on color strength, the K/S values and dye fixation rates of the fabrics printed under different steaming time conditions were evaluated, and the results are shown in Figure 7

As shown in Figure 7, as the steaming time increased, the K/S value of the interwoven fabric gradually increased and then decreased. When the steaming time was less than 15 min, the modified paste on the transfer printing paper was not completely swollen and the dye was not completely dissolved;

further, the gaps between the fibers of bio-based nylon 56 and cotton fabrics could not be fully expanded, and the color-fixing reaction was incomplete. Thus, the K/S value of the printed fabric was lower. When the steaming time was longer than 15 min, the degree of hydrolysis of the reactive dyes increased, and the K/S value of the fabrics and the fixing rate of the dyes decreased. Therefore, the steaming time was set at 15 min.

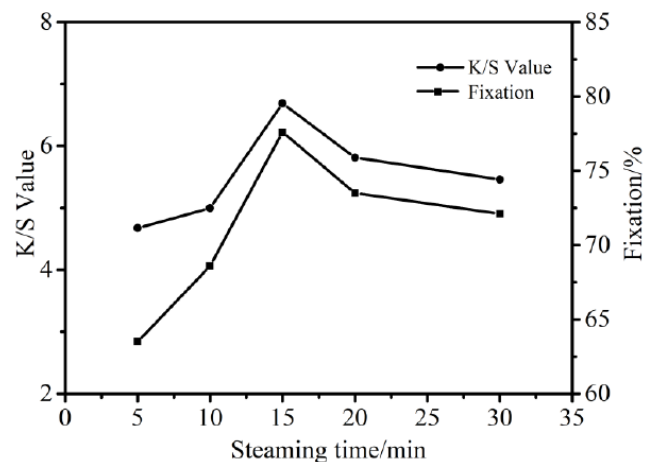


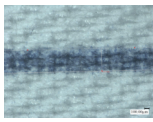
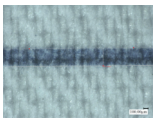
**Figure 7:** Effect of steaming time on the K/S value and fixation rate

### 3.3. Color Fastness and Outline Clarity of Printed Fabrics

The optimized transfer printing process was selected, and the following transfer printing conditions were used for printing patterns on bio-based nylon 56 and cotton interwoven fabrics: hot pressing at 130 °C under 3MPa pressure, steaming at 102 °C, steam saturation of 75%, steaming time of 15min. Then, the color fastness and outline clarity of the printed patterns on the fabrics were evaluated; the results are presented in Table 2. The renderings of the printed fabrics are shown in Figure 8, and scanning electron microscopy (SEM) images of the two types of fabrics are shown in Figure 9.

Table 2 reveals that, after the transfer printing of bio-based nylon 56 and cotton interwoven fabrics with Annosol Reactive Blue DS as the colorant, the color fastness to soaping and rubbing of the interwoven fabrics were both of grade 3–4 and above. Figure 8-(a) shows the pattern printed on the transfer printing paper, and Figure 8-(b) shows the effect on the interwoven fabric after transfer printing. The results clearly suggest that the method used in this study can meet the color fastness requirements of printed fabrics; at the same time, the technique provides a good outline definition and transfer printing effect and has good

**Table 2: Color Fastness and Line Widths of Transfer-Printed Fabrics**

Sample	Washing		Change	Rubbing		line width ( $\mu\text{m}$ )	
	Staining			Dry	Wet	Warp	Weft
	Cotton	Polyamide					
Blue	3-4	4	3-4	4	3-4	521.53	411.24

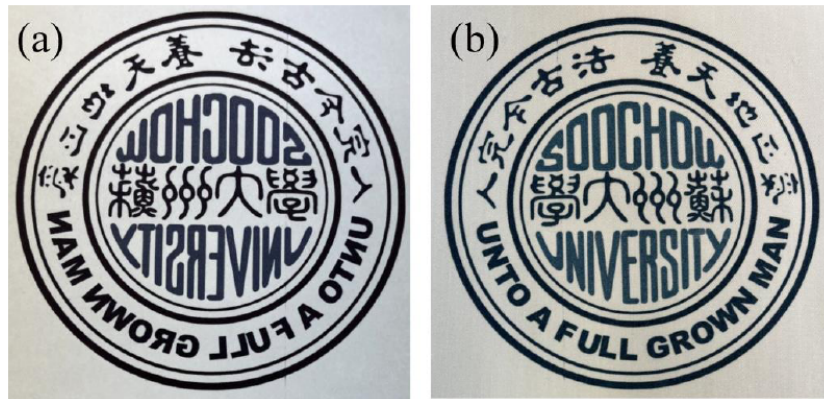


**Figure 8:** Rendering of transfer printing: (a) transfer printing paper; (b) interwoven fabric.

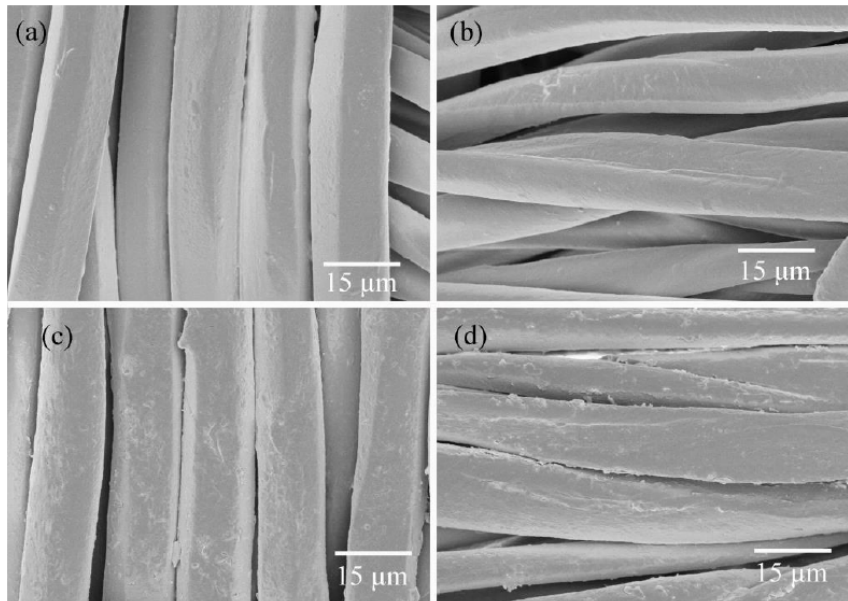


**Figure 9:** SEM images of the fabrics: (a) and (b) pre-printed bio-based nylon 56 and cotton fabrics, respectively; (c) and (d) printed biological nylon 56 and (d) cotton fabrics, respectively.

practicability. Figures 9-(a) and 9-(b) show the SEM images of the pre-printed bio-based nylon 56 and cotton fabrics, respectively, revealing that the fibers have a smooth surface with no discernible spots, and Figures 9-(c) and 9-(d) show the SEM images of the printed bio-based nylon 56 and cotton fabrics, respectively. Both bio-based nylon 56 and cotton fibers were effectively dyed with the reactive dye.

#### 4. CONCLUSIONS

An ink was formulated using Annosol Reactive Blue DS as the colorant for inkjet printing, and the transfer printing of the ink pattern on bio-based nylon 56 and cotton interwoven fabrics was optimized. The optimal hot-pressing conditions are as follows: hot-pressing temperature and pressure of 130 °C and 3 MPa,

respectively, steamer temperature of 102 °C, 75% steam saturation, and 15 min of steaming. After transfer printing using a transfer printing paper, the color fastness of the dyed fabrics to soap wash and rubbing of the interwoven fabric was determined to be of grade 3-4 and above. Moreover, the outline definition is better, and the method has good practical applicability.

## CONFLICTS OF INTEREST

The authors declare that they have no known competing financial interests or personal relationships that may have influenced the work reported in this paper.

## ACKNOWLEDGMENTS

This research was funded by Key Research and Development Plan of Jiangsu Province (BE2019001); Fund of National Innovation Center of Advanced Dyeing and Finishing Technology (ZJ2021A02); the Foundation of Jiangsu Engineering Research Center of Textile Dyeing and Printing for Energy Conservation, Discharge Reduction and Cleaner Production (Q811580722).

## REFERENCES

- [1] Draths K M, Frost J W. Environmentally compatible synthesis of catechol from D-glucose. *Journal of the American Chemical Society*, 2002, 117(9): 2395-2400. <https://doi.org/10.1021/ja00114a003>
- [2] Zhang Longgui, Ji Wenxi, Li Juan. Preparation and application of bio-based PA. *China Synthetic Resin and Plastics*, 2017, 34(2): 86-91.
- [3] Wu Quande, Hao Yuanzeng. Property and application of new engineering plastics nylon 46. *Engineering Plastics Application*, 2000(11): 31-33.
- [4] Wang Wanjie, Wang Yudong, Liu Mingying, Zhao Qinxiang, Ren Yanrong, Guo Ke, Li Xiangkui. Study on the crystallization kinetics of flexible and toughness PEFA 1212 under the constant cooling rate conditions. *Polymer Materials Science & Engineering*, 2002, 18(4): 158-161.
- [5] Lu Chengde. Structure and performance testing analysis of nylon 56 fiber. *Chemical Fiber & Textile Technology*, 2017, 46(3): 42-46.
- [6] Qi Yanbin, Ma Weichao, Chen Kequan. Production of 1,5-pentanediamine from lysine fermentation broth catalyzed by *Escherichia coli* whole cell. *Chemical Industry and Engineering Progress*, 2017, 36(5): 1843-1847.
- [7] Pardal F, Salhi S, Rousseau B, Tessier M, Claude S, Fradet A. Unsaturated polyamides from bio-based Z-octadec-9-enedioic acid[J]. *Macromolecular Chemistry and Physics*, 2008, 209(1): 64-74. <https://doi.org/10.1002/macp.200700319>
- [8] Li Mengmeng, Hu Liu, Hou Aiqin, Xie Kongliang. Development of dyeing property of Bio-based Nylon 56. *Dyestuffs and Coloration*, 2016, 53(05): 25-30.
- [9] Wu Tiantian, Wang Xueli, Yu Jianyong, Gao Yu, Liu Xiucui, Li Naiqiang. Study on Isothermal Crystallization Kinetics Bio-based Nylon 56. *Synthetic Fiber in China*, 2017, 46(2): 1-5-26.
- [10] Li Qing, Miao Sainan, Xing Tieling, Chen Guoqiang. Rheology and morphology of thickeners in textile transfer printing. *Journal of Textile Research*, 2015, 36(9): 75-81.
- [11] Li Qing, Xing Wang Yong, Xing Tieling, Chen Guoqiang. Properties of novel reactive transfer printing of silk. *Journal of Donghua University(English Edition)*, 2013, 30(6): 514-520.
- [12] Li Qing, Xing Tieling, Chen Guoqiang. Novel transfer printing paper for silk printing with reactive dye. *Materials Research Innovations*, 2014, 18: 879-885. <https://doi.org/10.1179/1432891714Z.000000000506>
- [13] Miao Sainan, Li Qing, Xing Tieling, Chen Guoqiang. Outline sharpness of cotton reactive prints with dye dry-heat transfer printing. *Dyeing & Finishing*, 2014, 40(21): 5-8+14.
- [14] Zhang Yu, Gan Chengyong, Chu Runshan, Xing Tieling, Chen Guoqiang. Dry-transfer printing of polyester/cotton fabric with disperse and reactive dye. *Dyeing & Finishing*, 2020, 46(5): 13-18.
- [15] Ma Xuesong, Gao Yi, Chen Ying, Jiang Yu, Zhu Feishi, Mei Tingjie. Dyeing performance of bio-based nylon PA56 with reactive dyes. *Dyeing & Finishing*, 2019, 45(18): 9-13-29.
- [16] Liu Li, Wang Liang, Wang Yifei, Chen Haisheng, Chai Lei, Yang Zheng, Tan Chuqing. Test and analysis on the thermal properties of microencapsulated phase change material suspension using propanol/water solution as base fluid. *Journal of Functional Materials*, 2014, 45(1): 1109-1113.
- [17] Jia Chunjiang, Chen Guangxue, Li Xiaozhou, Zhao Lei. Research on the application of water based ink in rotogravure printing. *Packaging Journal*, 2011, 3(1): 32-35-5.
- [18] Wang Zhenning, Tang Zhenyu. Numerical simulation of the effect of liquid surface tension and viscosity on the droplet formation of piezoelectric ejection. *Packaging Engineering*, 2010, 31(13): 24-27.

Received on 29-04-2023

Accepted on 25-05-2023

Published on 21-06-2023

DOI: <https://doi.org/10.12974/2311-8717.2023.11.01>

© 2023 Chu *et al.*

This is an open access article licensed under the terms of the Creative Commons Attribution Non-Commercial License (<http://creativecommons.org/licenses/by-nc/3.0/>) which permits unrestricted, non-commercial use, distribution and reproduction in any medium, provided the work is properly cited.